

We are IntechOpen, the world's leading publisher of Open Access books Built by scientists, for scientists

6,900

Open access books available

185,000

International authors and editors

200M

Downloads

Our authors are among the

154

Countries delivered to

TOP 1%

most cited scientists

12.2%

Contributors from top 500 universities



WEB OF SCIENCE™

Selection of our books indexed in the Book Citation Index
in Web of Science™ Core Collection (BKCI)

Interested in publishing with us?
Contact book.department@intechopen.com

Numbers displayed above are based on latest data collected.
For more information visit www.intechopen.com



Ligands and Coordination Compounds Used as New Photosensitized Materials for the Construction of Solar Cells

Yenny Patricia Avila Torres

Abstract

Ligand with conjugated π systems presents high planar and delocalized electronic density, which allows it to capture the radiations with an energy interval of wavelengths between 400 and 600 nm. The ligands can be linked to inorganic materials favoring the interchange in the system. Lewis acids improve the electronic distribution between donor and acceptor favoring the optical and electronic properties, yielding superior efficiencies. In this chapter, the evolution of the ligands such as Porphyrins, Metal-free organic dyes, and Ruthenium complexes used, and the construction of solar cells is described. In this context, three different small-molecule acceptors-donors are reported; *o*-PDT, *m*-PDT and *p*-PDT, based on phenyldiamine (PD) as spacer, and Thiazole (T) were designed and synthesized. There were estimated electronic, optical and photovoltaic parameters for these molecules. The interaction energies of functional groups for PD and T molecules, with DFT/B3LYP method, gas phase with 6-31g (d, 2p) basis sets, were represented and computed. The best photovoltaic parameters were described for *p*-PDT with PCE 26.18%, $J_{sc} = 14.79 \text{ mAcm}^{-2}$ and $\Delta E = 2.66 \text{ eV}$. The metal ion influences the electronic properties and decreases the ΔE GAP. The incorporation of the transition metals into hyperconjugated systems provides rigidity and effects of electronic back donation.

Keywords: photovoltaic cells, semiconductor, coordination compounds, dye-sensitized

1. Introduction

The current environmental problems and the energy crisis have led to creating new technologies. The renewable energies such as: biofuels, biomass, wind, geothermal, hydraulic, solar, tidal, among others become the main source of the energy generation. The use of solar cells represents an alternative among renewable energies. The development of new materials goes from inorganic structures until polymers, small molecules as organic photovoltaic (OPV) and photosensitized organic materials [1].

In this context, the discovery of ultrafast charge transfer between the semiconductor polymer and inorganic semiconductors have allowed that the OPV have

passed in a decade of values close to 1% of efficiency until exceeding 10% [2]. This rapid evolution is motivated by its high potential for generating flexible, lightweight and low cost panels changing the classic concept of panels photovoltaic. In the case of the traditional polymers, the electrons are highly localized and require great energy to be excited (>5 eV) converting them into electrical insulators. In contrast, in conjugated polymer and structures the electrons from π orbitals form π -type bonds that are associated with lower energies, corresponding to the range of ultra-violet and visible radiation. In molecular solids the transition $\pi \rightarrow \pi^*$ that occurs between the occupied molecular orbital of higher energy (HOMO) and the lower energy of orbital (LUMO) determine the equivalent to the forbidden band energy of inorganic semiconductors [3, 4]. On the other hand, they had developed sensitized cell from organic dyes. These are also called Grätzel cells. Photoelectrons that introduce into the conduction band of TiO_2 that works as a semiconductor, under light illumination [5].

Dye-sensitized cell (DSSC) have been developed as functional biomimetic models of biological process. In the nature exists dyes with electronic properties that allows to purpose design news in solar panel. Chlorophyll, constituted an example in where there is light absorption and charge-carrier transport. The organic molecule is coupled to semiconductor enhancing the Gap band. This electronic transfer promote absorption to the visible region, which increase its applications [6].

The researchers in a world context have designed, developed and synthesized ruthenium complexes, porphyrins, metal-free organic dyes and organic molecules in this field.

1.1 Ruthenium complexes

The efficiency of DSSC depends on different requirements listed below [7, 8]:

- i. Broad and strong absorption, preferably extending from energies greater than 900 nm.
- ii. The dye needs to be photochemically, thermally, and electrochemically robust within the DSSC in order to withstand the harsh conditions of a practical module.
- iii. Firm, irreversible adsorption to the semiconductor's surface (TiO_2) and strong electronic coupling between its excited state and the semiconductor conduction band.
- iv. Reduction potential is sufficiently higher than the semiconductor conduction band Edge in order to enable charge injection.
- v. Chemical stability in the ground and the excited states for rapid dye regeneration and charge-injection processes.

Different types of dyes have been tested in the DSSC setting, including: transition-metal complexes, organic dyes, porphyrins and phthalocyanines [9–12]; however, in terms of photovoltaic performance and long-term stability, Ru(II) complexes comprise the most successful family of DSSCs sensitizers, shown in **Table 1**. A study on these champion dyes reveals that majority are derivate of **N3**. The **N3** dye represents the first high-performance Ru(II) sensitizer reported in 1993 by Grätzel and co-workers [13], affording power conversion efficiencies of 10.3%. The chemical modification of **N3** and **N719** is made possible because only two

anchoring groups are necessary for electron injection [14, 15] thus various functional groups can be installed to block the electrolyte from interacting with the surface or absorb more light. Then, the performance of these successful sensitizers encompasses ligands that combine extended π -conjugated systems, aspiring to enhance the optical absorptivity of the semiconductor's surface, along with long hydrophobic alkyl chains, aiming an increase of tolerance against water attack (**Table 1**). Equally importantly **N719**, which essentially differ only in the protonation state of tetra-protonated parent dye **N3**, afford a nearly quantitative conversion of incident photons into electric current over a large spectral range. The improved efficiency of **N719**, was mainly attributed to the increased cell voltage. Since 1993, chemical modifications of these early Ru(II) complexes have led to researchers achieving power conversion efficiencies up to 11.7% (**C106** dye) [16–24], where one of the DCBPy ligands has been replaced with an extended conjugation using thiophenes and long alkyl chains, lastly, these prevents interfacial recombination [25].

1.2 Porphyrins

The so-called solar cells sensitized by a dye are a type of hybrid devices that have reached a higher degree of development so far. Within his field, porphyrins represent a very interesting alternative because there is efficient model harnessing sunlight. These systems can be synthesized in bulk heterojunction (BHJ) organic solar cells. The interaction of macrocycles with metal ions such as: Fe^{2+} , Fe^{3+} , Co^{2+} , Co^{3+} , Ni^{2+} , Zn^{2+} , Cu^{2+} , Ru^{2+} , Pd^{2+} and Pt^{2+} and hydrogen, alkyl, cycloalkyl, cyclohexyl, cycloheptyl, cyclooctyl, haloalkyl, perhaloalkyl, ether chains have permitted the stabilizations of promising new collections. In dye-sensitized solar porphyrin-based push-pull.

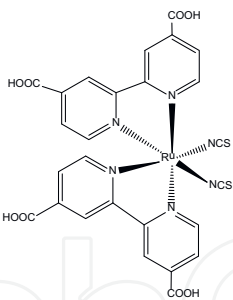
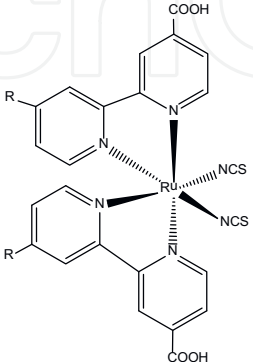
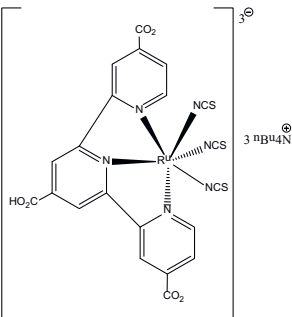
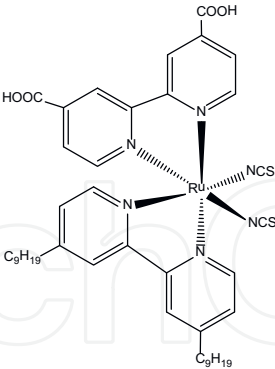
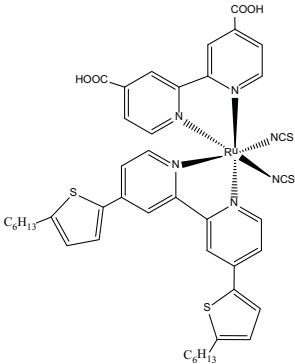
photosensitizers have demonstrated their potential as large and rigid planar conjugated structures, which enhance p-electron delocalization and promote intermolecular π - π interaction, as well charge transport in devices. A problem that they can presents is the effect by lack of light-harvesting beyond 850 nm, thus limiting their cell performance. In the papers, it has been reported that 50% of the total solar phonon flux is located in the red and near-infrared spectra. Zhu and colleagues had reported in 2016 that is quite urgent to develop efficient NIR absorbing molecules for high performance organic solar cells. In the next table, the authors show different publications about the development of new bioinspired porphyrin materials (**Table 2**).

1.3 Metal-free organic dyes

The DSSC free organic dyes are sensitized molecules whose perspective are aimed at staking, on top of one other in order to obtain panchromatic absorption. **Table 3** shows azo, cyano, thiophene, and carbonyl with highly conjugated. A PCE value at 14.7 has been reported by Kakiag et al. [49]. The PCE increase with V_{oc} and J_{sc} and the best properties were associated with carboxylic group and highly polarizability in the presence of nitrile group.

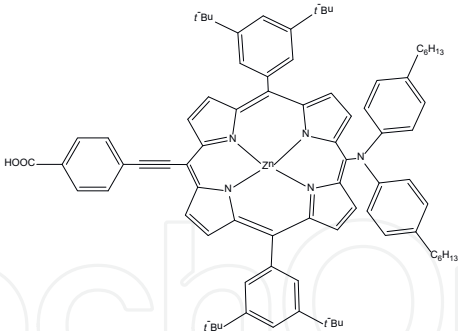
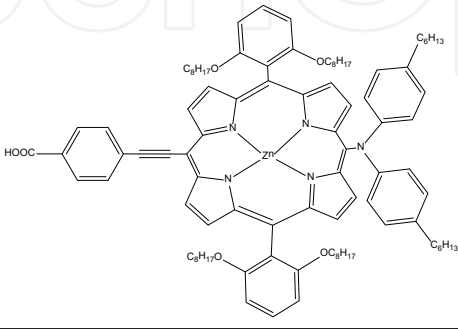
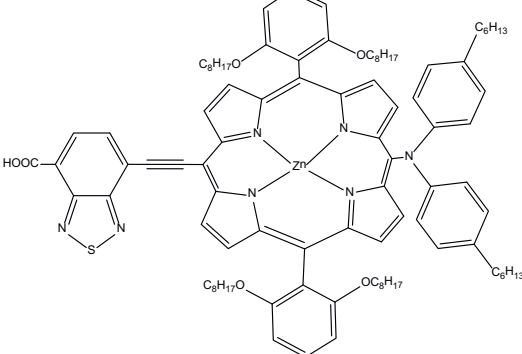
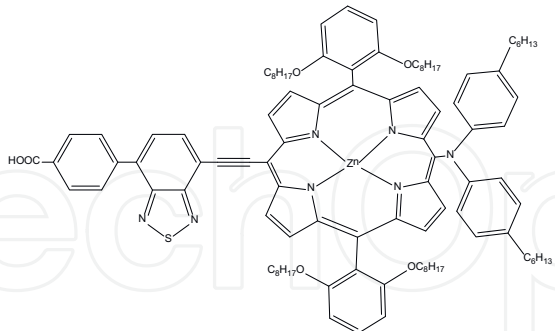
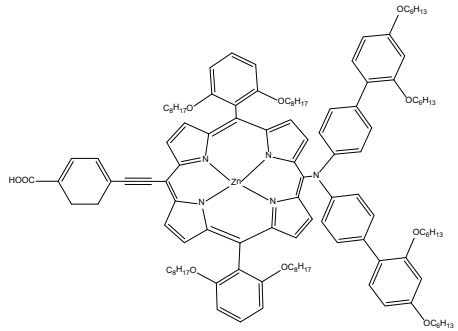
The extension of the conjugated chain and the substitution of the thiophene groups do not represent a marked difference that allows concluding a relationship between the photovoltaic properties and the structure.

Therefore, this article reports the bibliographic revision for these compounds, specifying the following parameters: Chemical name, abbreviation, structure, power conversion efficiencies (PCE), J_{sc} (short-circuit-current), V_{oc} (open circuit voltage) electrolyte used and authors.

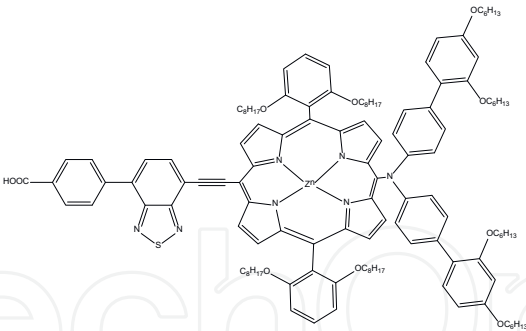
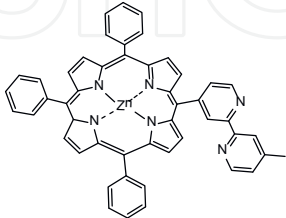
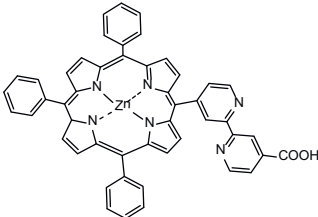
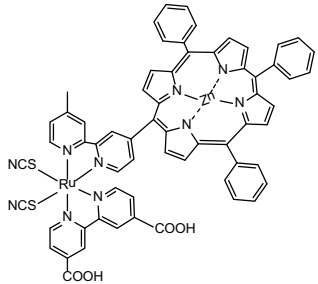
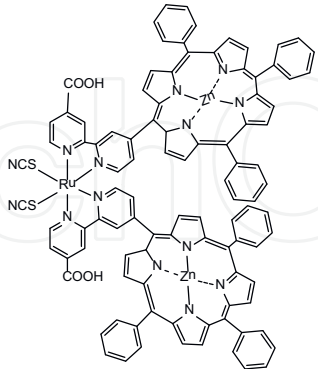
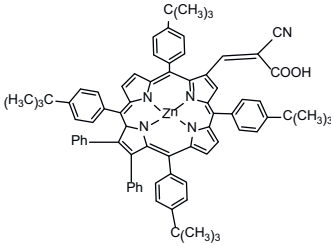
Chemical name	Author's designation	Structure	PCE (%)	J _{sc} (mA/cm ²)	V _{oc} (mV)	Electrolyte
<i>cis</i> -Bis (isothiocyanato)bis (2,2'-bipyridyl-4,4'-dicarboxylato) ruthenium(II)	N3		10.3	7.9	660	I ₃ /I ⁻
Di-tetrabutylammonium <i>cis</i> -bis (isothiocyanato)bis (2,2'-bipyridyl-4,4'-dicarboxylato) ruthenium(II)	N719		11.18	17.73	846	I ₃ /I ⁻
[(C ₄ H ₉) ₄ N] ₃ [Ru-(Htcterpy) (NCS) ₃] (tcterpy) 4,4',4''-tricarboxy-2,2',2''-terpyridine	Black dye		10.4	20	720	I ₃ /I ⁻
<i>cis</i> -Ru (4,4'-dicarboxylic acid-2,2'-bipyridine) (4,4'-dinonyl-2,2'-bipyridine) (NCS) ₂	Z907		9.5	12.5	730	
<i>cis</i> -Bis(isothiocyanato) (2,2'-bipyridyl-4,4'-dicarboxylato) (4,4'-bis(5-hexylthiophen-2-yl)-2,2'-bipyridyl) ruthenium(II), Ruthenate(2-), [[2,2'-bipyridine]-4,4'-dicarboxylato (2-)-N1,N1'] [4,4'-bis(5-hexyl-2-thienyl)-2,2'-bipyridine-N1, N1'] bis(thiocyanato-N)-, hydrogen (1:2)	C101		11	17.9	778	I ₃ /I ⁻

Chemical name	Author's designation	Structure	PCE (%)	J _{sc} (mA/cm ²)	V _{oc} (mV)	Electrolyte
TBA(Ru[(4-carboxylic acid-4'-carboxylate-2,2'-bipyridine)(Ligand-11)(NCS) ₂])	CYC-B11		11.5	20.05	743	I ₃ /I ⁻
—	C106		11.7%	19.8	758	I ₃ /I ⁻
—	GS3		2.79	9.78	435	I ₃ /I ⁻
—	NCSU-10		8.34	18.2	703	I ₃ /I ⁻
—	Complex 16		1.26	4.53	496	I ₃ /I ⁻
—	[Ru]2		6.45	13.48	650	—
—	[Ru]3		5.23	11.77	598	—
—, it is not mentioned in the article.						

Table 1.
Ruthenium complexes for DSSC [26–33].

Chemical name	Author's designation	Structure	PCE (%)	J _{sc} (mA/cm ²)	V _{oc} (mV)
—	YD2		10.9	18.6	770
—	YD2-o-C8		12.3	17.3	965
—	GY21		2.5	5.03	615
—	GY50		12.75	18.53	885
—	SM371		12	15.9	960

On the other hand, in this research also have been reported the theoretical studies towards the effect the spacer molecule in macrocycles. The linear molecule

Chemical name	Author's designation	Structure	PCE (%)	J _{sc} (mA/cm ²)	V _{oc} (mV)
—	SM 315		13	18.1	910
—	A4		0.05	0.09	330
—	A6		0.28	0.83	480
—	A7		0.38	1.33	450
—	A8		0.05	0.26	370
—	ZnT(Mes) P(CN-COOH)		3.15	7.8	575

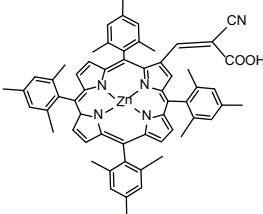
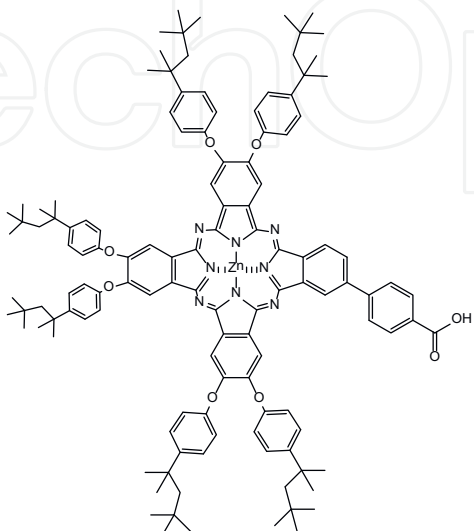
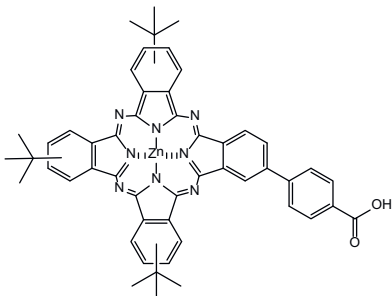
Chemical name	Author's designation	Structure	PCE (%)	J _{sc} (mA/cm ²)	V _{oc} (mV)
—	ZnT(4-t-Bu)P(Ph ₂) (CN-COOH)		1.72	4.3	580
—	ZnPc1		0.73	2.26	530
—	TT1		1.54	3.98	550
—, it is not mentioned in the article.					

Table 2.
Porphyrins for DSSC [34–40].

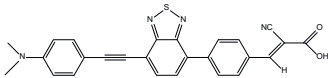
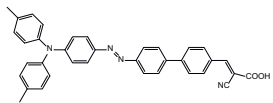
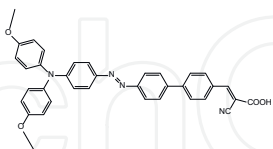
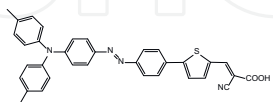
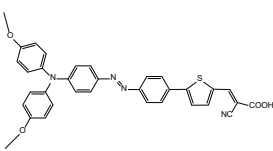
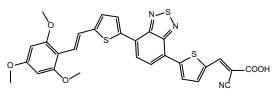
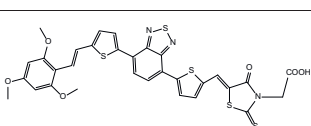
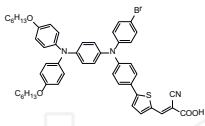
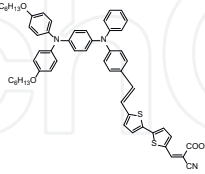
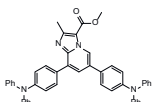
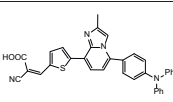
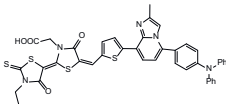
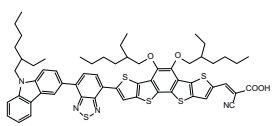
designed was a benzothiophene derivate (T) and the spacer selected were *o*-*m* or *p*-diphenyldiamine. The spacer represented the communication channel between linear chains, denominated T. The stabilization of the macrocycles depends of the good assembly. The authors reported a study relationship with the photovoltaic properties for three macrocycles in function of isomeric effect in the spacer. The calculations were performed using Gaussian 09 16-18, program with B3LYP functional [58–61] and 6-31-6 (d, 2p) as basis set [64] in order to investigate the molecular geometry, electronic structures, and optical properties of *o*-PDT, *m*-PDT and *p*-PDT (**Figure 1**).

The stationary point was estimated with level of theory reported previously for the authors [64]. Finally, the authors through the Lewis acid incorporation showed an electronic improvement mechanism. The acid Lewis effect, as evaluated considering the tetracoordinated mode around metal center (**Figure 2**).

Chemical name	Author's designation	Structure	PCE (%)	J _{sc} (mA/cm ²)	V _{oc} (mV)	Electrolyte
2-Cyano-7-(1,1,6,6-tetramethyl-10-oxo-2,3,5,6-tetrahydro-1H,4H,10H-11-oxa-3a-aza-benzo[de]anthracen-9-yl)-hepta-2,4,6-trienoic acid	NKX-2586		3.5	15.1	470	—
2-Cyano-5-(1,1,6,6-tetramethyl-10-oxo-2,3,5,6-tetrahydro-1H,4H,10H-oxa-3a-aza-benzo[de]anthracen-9-yl)-penta-2,4-dienoic acid	NKX-2311		6.0	14.0	600	—
2-Cyano-3-[5'-(1,1,6,6-tetramethyl-10-oxo-2,3,5,6-tetrahydro-1H,4H,10H-11-oxa-3a-azabenz[de]anthracen-9-yl)-[2,2']bithiophenyl-5-yl]acrylic acid	NKX-2677		7.7	14.3	730	—
—	D5		5.1	11.9	660	—
2-cyano-3-{5'-[1-cyano-2-(1,1,6,6-tetramethyl-10-oxo-2,3,5,6-tetrahydro-1H,4H,10H-11-oxa-3a-aza-benzo[de]anthracen-9-yl)-vinyl]-[2,2']bithiophenyl-5-yl}-acrylic acid	NKX-2883		7.3	16.90	580	—
5-[[4-[4-(2,2-Diphenylethenyl)phenyl]-1,2,3,3a,4,8b-hexahydrocyclopent[b]indol-7-yl]methylene]-2-(3-octyl-4-oxo-2-thioxo-5-thiazolidinylidene)-4-oxo-3-thiazolidineacetic acid	D205		9.52	18.7	710	Ionic-liquid
2-Cyano-3-[5'-[2-[4-[N,N-bis(4-(2-ethylhexyloxy)-phenyl)amino]phenyl]-3,4-ethylenedi-oxythiophene-5-yl]-3,3'-di-n-hexylsilylene-2,2'-bithiophene-5-yl]acrylic acid	C219		8.9	17.94	770	I ₃ /I ⁻
—	C218		8.95	15.8	768	I ₃ /I ⁻

Chemical name	Author's designation	Structure	PCE (%)	J _{sc} (mA/cm ²)	V _{oc} (mV)	Electrolyte
2-cyano-3-[5'-(1,1,6,6-tetramethyl-10-oxo-2,3,5,6-tetrahydro-1H,4H,10H-11-oxa-3a-aza-benzo[de]anthracen-9-yl)-[2,1,3-benzothiadiazole]-4-thiophen-2-yl]-acrylic acid	HKK-CM4		5.97	14.3	580	—
2-cyano-3-[5'-(1,1,6,6-tetramethyl-10-oxo-2,3,5,6-tetrahydro-1H,4H,10H-11-oxa-3a-aza-benzo[de]anthracen-9-yl)-[2,1,3-benzothiadiazole]-4-(3,4-ethylene dioxothiophenyl-5-yl)]-acrylic acid	HKK-CM5		5.03	13.3	560	—
—	C228		4.7	7.6	830	Co ²⁺ /Co ³⁺
—	C228		4.4	7.78	760	I ₃ /I [−]
—	C229		9.4	15.3	850	Co ²⁺ /Co ³⁺
—	C229		6.7	15.20	680	I ₃ /I [−]
3-{6-[4-[bis (2',4'-dihexyloxybiphenyl-4-yl)amino-]phenyl]-4,4-dihexyl-cyclopenta-[2,1-b:3,4-b']dithiophene-2-yl]-2-cyanoacrylic acid	Y123		12.3	17.7	935	Co ²⁺ /Co ³⁺
—	ADEKA-1		11.2	19.11	783	I ₃ /I [−]
—	LEG 4		14.7	9.55	776	I ₃ /I [−]

Chemical name	Author's designation	Structure	PCE (%)	J _{sc} (mA/cm ²)	V _{oc} (mV)	Electrolyte
—	KNS-1		2.01	4.93	600	Co ²⁺ /Co ³⁺
—	KNS-2		2.95	6.92	650	Co ²⁺ /Co ³⁺
—	JM-2		6.5	14.4	620	I ₃ /I ⁻
3-(5-((3,6-bis(bis(4-methoxyphenyl)amino)-9H-fluoren-9-ylidene)methyl)thiophen-2-yl)-2-cyanoacrylic acid	TK-4		5.9	13.29	667	—
3-(5'-((3,6-bis(bis(4-methoxyphenyl)amino)-9H-fluoren-9-ylidene)methyl)-[2,2'-bithiophen]-5-yl)-2-cyanoacrylic acid	TK-5		7.5	17.85	653	—
3-(5'-((3,6-bis(bis(4-(octyloxy)phenyl)amino)-9H-fluoren-9-ylidene)methyl)-2,2'-bithiophen-5-yl)-2-cyanoacrylic acid	TK-6		7.8	17.19	663	—
—	O4T		5.07	10.7	630	—
—	ST4		6.73	14.4	640	—
—	P2		2.18	4.85	680	—
—	LS-385		2.68	6.33	582	I ₃ /I ⁻
—	LS-386		2.69	6.53	561	I ₃ /I ⁻

Chemical name	Author's designation	Structure	PCE (%)	J _{sc} (mA/cm ²)	V _{oc} (mV)	Electrolyte
—	LS-387		5.61	13.26	595	I ₃ /I [−]
—	TA1		2.56	5.40	662	—
—	TA2		3.45	6.83	704	—
—	TA3		3.69	7.81	654	—
—	TA4		4.78	9.92	662	—
(Z)-2-cyano-3-(5''-(E)-2,4,6-trimethoxystyryl)-[2,2':5',2''-terthiophen]-5-yl) acrylic acid	MR-5		6.03	15.27	610	—
2-((Z)-4-oxo-2-thioxo-5-((5''-(E)-2,4,6-trimethoxystyryl)-[2,2':5',2''-terthiophen]-5-yl) methylene) thiazolidin-3-yl) acetic acid	MR-6		3.2	8.7	560	—
—	D6		4.7	8.6	793	Co ²⁺ /Co ³⁺
—	D7		4.0	8.2	768	Co ²⁺ /Co ³⁺
—	SP1		0.86	2.59	625	—
—	SP3		0.43	2.31	532	—
—	SP4		0.58	0.78	290	—
—	BD-3		5.46	12.21	680	I ₃ /I [−]

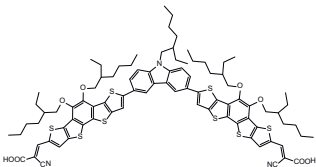
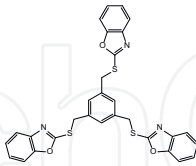
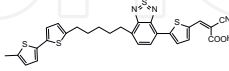
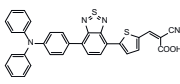
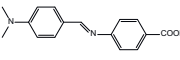
Chemical name	Author's designation	Structure	PCE (%)	J _{sc} (mA/cm ²)	V _{oc} (mV)	Electrolyte
—	BD-5		5.34	12.23	680	I ₃ /I ⁻
—	Dendrimer 1		5.19	13.00	675	I ₃ /I ⁻
—	4a		0.95	2.60	500	—
—	4b		4.51	9.36	630	—
—	N, N'-PABA		1.00	2.72	537	I ₃ /I ⁻
—, it is not mentioned in the article.						

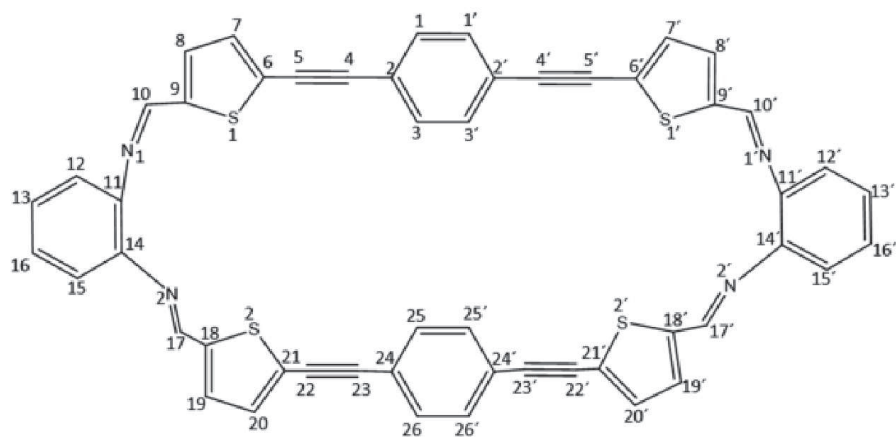
Table 3.
Structures associated with metal-free organic dyes [41–63].

2. Material and methods

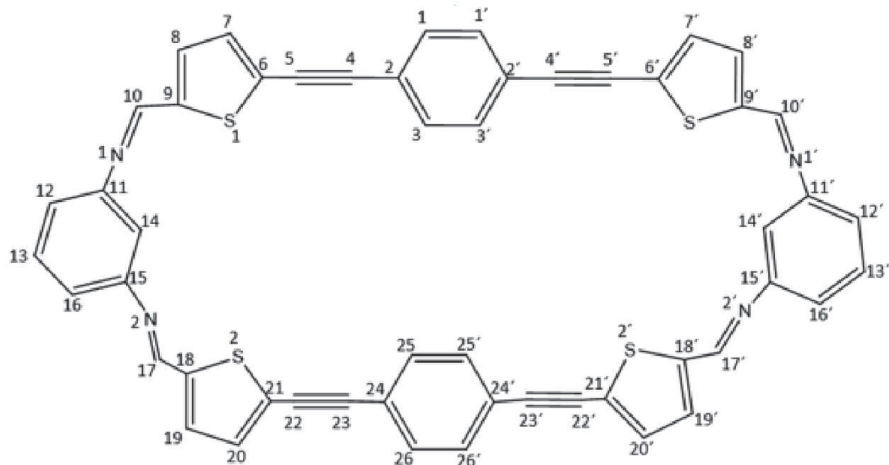
2.1 Method theoretical

To explore and understand the electronic and optoelectronic properties of photosensitized materials with application in OPV technology, many theories have emerged. One of the most important and common theories is the theory of functional density (DFT), which is a tool that allowed to establish any property used in photosensitized materials, quantum state of atoms, molecules and solids, making modeling and simulation possible of complex systems with millions of degrees of freedom. At present, DFT has grown tremendously and has become one of the main tools in theoretical physics and molecular chemistry. Modeling in the framework of computational chemistry of photosensitized systems made up of electron donors and electron acceptors ultimately influences photo induced electron transfer and energy reactions. Numerous studies using the Density Functional Theory (DFT) methodology to design, evaluate and predict photovoltaic properties of photoactive materials with application in OPV have been published. The approximation of the theory of functional density (DFT) implemented was Gaussian 09 together with the functional correlation (B3LYP) and the base set 6-31g (d, 2p). This calculation allows optimization of geometry without symmetry restrictions for stationary points. In addition, it provided information on the harmonic frequency analysis, which allows the optimized minimum to be verified. The local minimum is identified when the number of imaginary 32 frequencies is equal to zero.

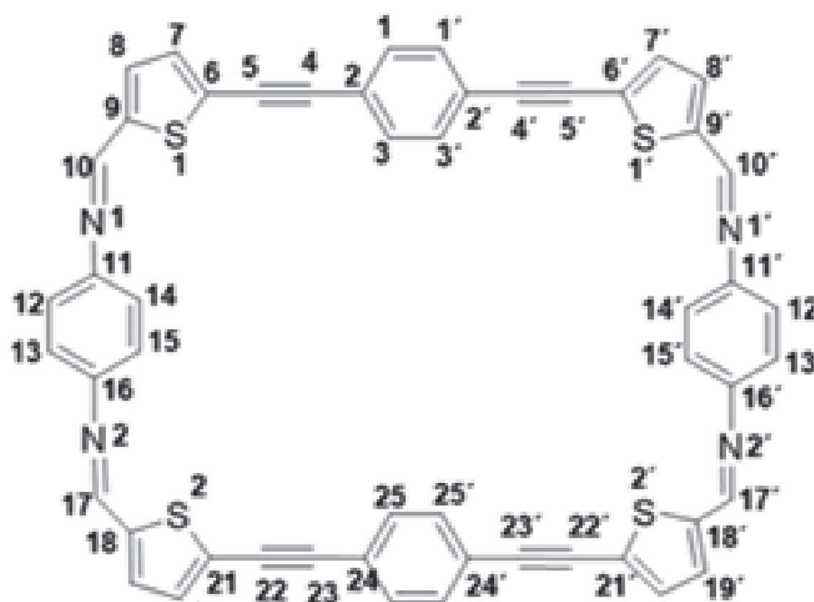
The analysis of the changes in electron density for a given electronic transition was based on the electron density difference maps (EDDMs) constructed using the GaussSum suite of programs. Gásquez and co-workers had proposed two different electronegativities (X) for the charge transfer process: one that describes fractional



(a)



(b)



(c)

Figure 1.
Chemical structure for (a) p-PDT, (b) m-PDT and (c) o-PDT.

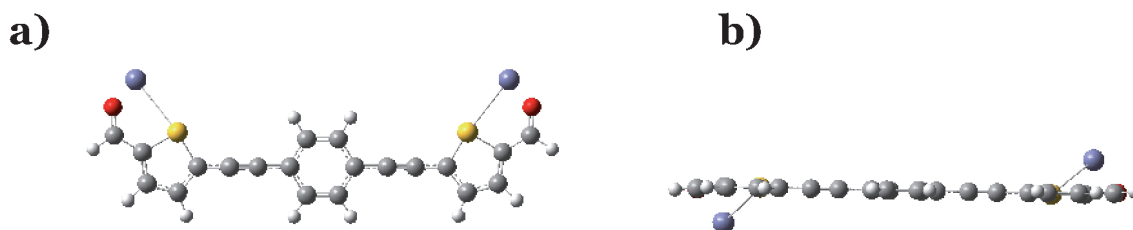


Figure 2.
Geometry optimization for (a) T and (b) TZn.

negative charge donation X^- whereas the other gives the fractional negative charge acceptance X^+ , Eqs. (1) and (2):

$$X^- = 0.25(3I + A) \quad (1)$$

$$X^+ = 0.25(I + 3A) \quad (2)$$

Thus, the construction of a so-called donor-acceptor map (DAM) has been suggested. A DAM graphic can be constructed by plotting the values of (y-axis) and X^+ (x-axis) for each molecule of interest.

The photovoltaic properties are calculated according to the Scharber model, which is an empirical model for predicting the PCE of organic cell solar. HOMO-LUMO as orbital border under solar irradiation with AM 1.5 G (ASTM G173). The PCE was expressed by the following Eqs. (3) and (4), in where V_{oc} is the open circuit voltage, and J_{sc} is short circuit current.

$$PCE = FF \left(J_{sc} \frac{V_{oc}}{P_{inc}} \right) \quad (3)$$

where FF is a fill factor of 0.75, Eq. (4):

$$J_{sc} = q \int_{\lambda_{min}}^{\lambda_{max}} EQE \phi^{AM\ 1.5\ G}(\lambda) d\lambda \quad (4)$$

(q = elementary charge, EQE = external quantum efficiency, ϕ = irradiation flow with AM 1.5 G, and λ = wavelength), and P_{inc} (incident light power).

On the other hand, the valor corresponding ΔE_{GAP} was calculated as, Eq. (5):

$$\Delta E = E(LUMO) - E(HOMO) \quad (5)$$

LHE (light capture efficiency determinate), (f = oscillator strength) and E_{s1} = Excitation energy for λ_{max} , Eq. (6).

$$LHE = 1 - 10^{-f} \quad (6)$$

3. Results and discussion

3.1 Optical properties of macrocycle molecules

The excitation energies (E_{s1}) presented in **Table 4** were relatively small for the PDT molecule ligand, which indicate a shift to visible region in relationship with λ_{max} . The *p*-PDT showed the lowest value for E_{s1} , which is directly correlated with the conversion energy (PCE). On the other hand, the cycle size generated for *o*-PDT

Molecule	Wavelength λ_{\max}	E_{s1} (eV)	F	LHE
<i>o</i> -PDT	432.68	2.874	2.0217	0.9905
<i>m</i> -PDT	425.37	2.923	2.8755	0.9987
<i>p</i> -PDT	465	2.67	0.07	0.14

Table 4.

Optical properties for (a) *o*-PDT, (b) *m*-PDT and (c) *p*-PDT.

and *m*-PDT systems is smaller, but this does not guarantee a better transfer. On the contrary, there is less efficient in the electronic transport.

The LHE values were 2.0217, 2.8755 and 0.07 for *o*-PDT, *m*-PDT and *p*-PDT, respectively. This indicates that *o*-PDT and *m*-PDT had a similar sensitivity to sunlight and will reflect higher values of LHE compared to *p*-PDT.

The visible light absorption ability may benefit from absorbing more photons and generating high photocurrent, which is a strong advantage of T derivatives. In the previous reports, PD spacers that cannot absorb visible light were observed. It is necessary that T derivate linked to the PD fragment enhances the electronic coupling in the excited state, which operates as a gated wire in π -conjugated systems, as is observed for *o*-PDT, *m*-PDT and *p*-PDT (**Figure 3**). The isomeric effect is greatly correlated to geometric distortion *o*-PDT and *m*-PDT molecules, which were dramatically affected in relationship to its planarity. The cavity between linear molecules is small, but the torsion affects the electronic properties.

3.2 Geometry study for macrocycles with Lewis acid.

The effect of Lewis acid on macrocycle stabilization is shown below. The geometric environment of the metallic center was tetrahedral, considering two positions to the electro donator atoms corresponding to linear and macrocycle molecule; and two water molecules. The incorporation of the metal into the linear chain (ZnT) generates a decrease in the value for GAP around 1.72 eV, a value located in the visible region. However, the effect is more severe when incorporated into the macrocycle, in where; its addition generated a decrease in GAP still 1.55 eV (*p*-ZnPDT). The DAM graphic for these systems indicated a significant improvement in donor capacity. These criteria are important to electronically activate the photovoltaic cell (**Figure 4**).

The spectra in **Figure 5** showed a similar profile for TZn, and *p*-ZnPDT with the incorporation of Lewis acid in the structure, which have an intense main band to 568 nm, and 516 nm respectively. This band corresponds to the dominant electron transition from HOMO to LUMO, that is, from the π molecular orbital (chromophore fragments- π -linker) to the π^* orbital (acceptor fragment), and this process can be ascribed to the intramolecular charge transfer.

3.3 Photovoltaic properties of macrocycle molecules

The results showed in **Table 5** suggested decreased the ΔE_{GAP} in relationship with PCE. These results are congruent with the optical, and electronic properties observed previously. The *p*-PDT presented the best photovoltaic properties. The metal ion generates a symmetrical tension in the system, and this could explain its behavior. The J_{sc} increased in function of decreased the ΔE_{GAP} , concluding that the preferential isomer for the construction of this family macrocycles is the *p*-PDT, considering theoretical models in the gas phase.

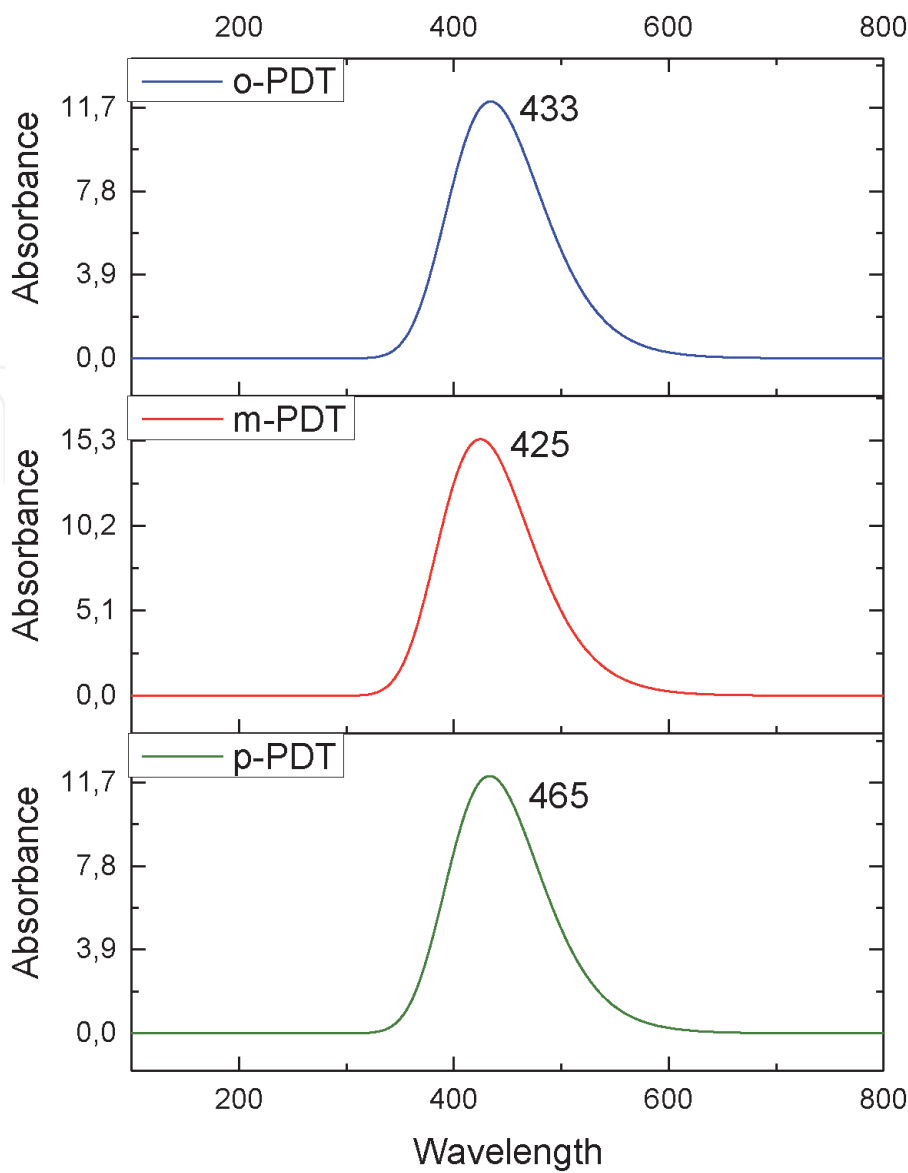


Figure 3.
Theoretical spectra electronic for (a) o-PDT m-PDT.

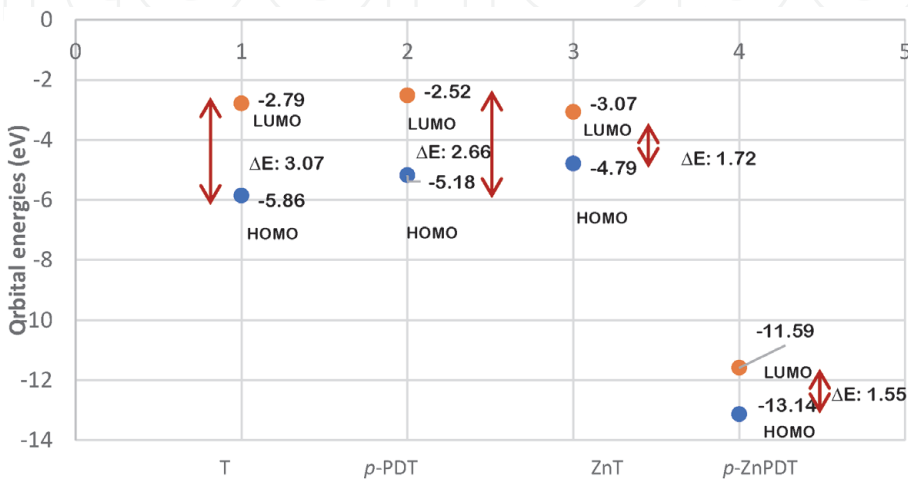


Figure 4.
DAM graphic for T, p-PDT, ZnT and p-ZnPDT.

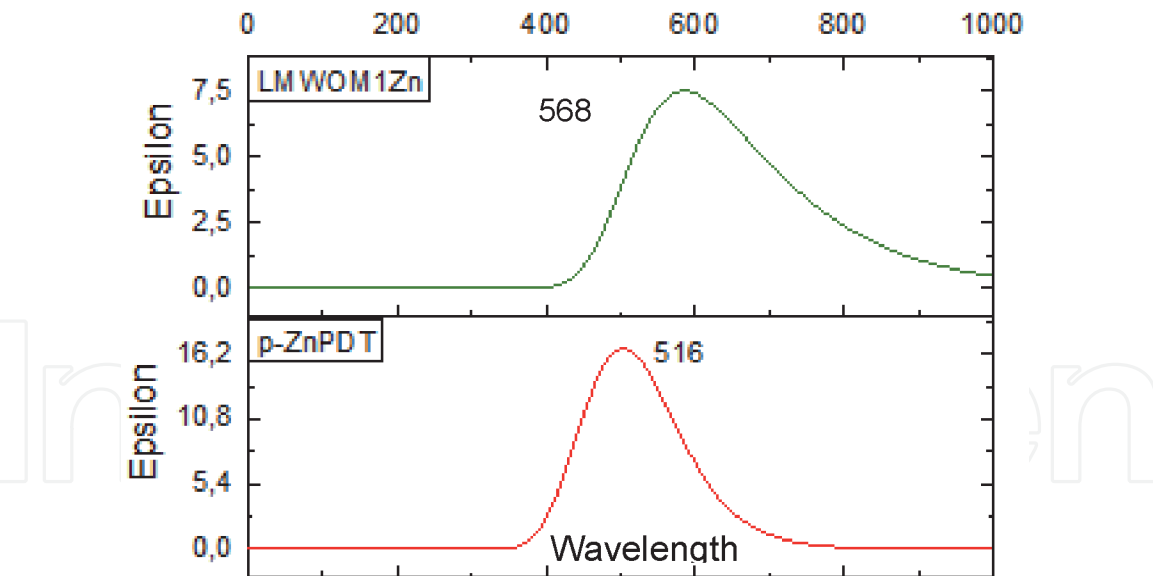


Figure 5.
Theoretical spectra electronic for TZn and p-ZnPDT.

Molecule	ΔE_{GAP} (eV)	J_{sc} (mA/cm ²)	V_{oc} (V)	FF	PCE (%)
T	3.07	5.36	2.77	0.75	11.12
p-PDT	2.66	14.79	2.36	0.75	26.18
ZnT	1.72	21.52	1.42	0.75	22.92
p-ZnPDT	1.55	11.76	1.25	0.75	11.02

Table 5.
Photovoltaic parameters for T, p-PDT, ZnT and p-ZnPDT.

4. Summary and future perspectives

The purpose of this review of DSSC materials was to compile the information reported to: synthesized ruthenium complexes, porphyrins, and metal-free organic dyes. For researchers, it is important to know parameters such as: PCE, J_{sc} , and V_{oc} ; which help you to diffuse between structures, and propose synthesis strategies that make possible new materials in this field application. Principles for the future development of new molecules can be analyzed and likewise it is interesting support to follow up structure families as a function of time. Although many structures are shown here, there is still a need to optimize the chemical, and physical properties to promote improved solar cells. On the other hand, in this work, the best photovoltaic parameters were described for p-PDT with PCE 26.18%, $J_{\text{sc}} = 14.79 \text{ mA/cm}^2$, and $\Delta E = 2.66 \text{ eV}$ such as macrocycle. The metal ion influences the electronic properties, and decreases the ΔE_{GAP} . The incorporation of Lewis acid in the structure macrocycle to increase of the optical properties, which allows rigidity that can benefit planarity.

Acknowledgements

This work was supported by Universidad Santiago de Cali—DGI Grants 63661. The author acknowledgment to Melissa Suarez for technical support and Hoover Valencia for data acquisition.

Conflict of interest

The authors declare that they have no conflict of interests.

IntechOpen

IntechOpen

Author details

Yenny Patricia Avila Torres
Research Group QUIBIO, Facultad de Ciencias Básicas, Universidad Santiago de
Cali, Santiago de Cali, Colombia

*Address all correspondence to: yavilatorres@gmail.com

IntechOpen

© 2020 The Author(s). Licensee IntechOpen. This chapter is distributed under the terms of the Creative Commons Attribution License (<http://creativecommons.org/licenses/by/3.0>), which permits unrestricted use, distribution, and reproduction in any medium, provided the original work is properly cited. 

References

- [1] Owusu PA, Asumadu-Sarkodie S. A review of renewable energy sources, sustainability issues, and climate change mitigation. *Cogent Engineering*. 2016; **3**(1):1167990
- [2] Wang P, Zakeeruddin SM, Moser JE, Humphry-Baker R, Comte P, Aranyos V, et al. Stable new sensitizer with improved light harvesting for nanocrystalline dye-sensitized solar cells. *Advanced Materials*. 2004;**16**(20): 1806-1811
- [3] Hara K, Sugihara H, Tachibana Y, Islam A, Yanagida M, Sayama K, et al. Dye-sensitized nanocrystalline TiO₂ solar cells based on ruthenium (II) phenanthroline complex photosensitizers. *Langmuir*. 2001;**17**(19):5992-5999
- [4] Manivel P, Mohana Roopan S, Nawaz Khan F. Synthesis of O-substituted benzophenones by Grignard reaction of 3-substituted isocoumarins. *Journal of the Chilean Chemical Society*. 2008; **53**(3):1609-1610
- [5] Philipps SP, Bett AW, Horowitz K, Kurtz S. Current Status of Concentrator Photovoltaic (CPV) Technology. No. NREL/TP-5J00-65130. Golden, CO (United States): National Renewable Energy Lab. (NREL); 2015
- [6] Dusastre V. Materials for sustainable energy: A collection of peer-reviewed research, and review articles. Editorial. Nature Publishing Group, World Scientific; 2011
- [7] O'regan B, Grätzel M. A low-cost, high-efficiency solar cell based on dye-sensitized colloidal TiO₂ films. *Nature*. 1991;**353**(6346):737
- [8] Mathews L, Tidwell C, Bharara P, Stephens G, Su T, Carter A. Copper 5, 10, 15, 20-Tetrakis-(3, 4-dibenzoyloxyphenyl) porphyrin. *Molbank*. 2017;**1**(2017):M931
- [9] Robertson N. Optimizing dyes for dye-sensitized solar cells. *Angewandte Chemie International Edition*. 2006; **45**(15):2338-2345
- [10] Xie P, Guo F. Molecular engineering of ruthenium sensitizers in dye-sensitized solar cells. *Current Organic Chemistry*. 2007;**11**(14):1272-1286
- [11] Bessho T, Zakeeruddin SM, Yeh C-Y, Diau EW-G, Grätzel M. Highly efficient mesoscopic dye-sensitized solar cells based on donor-acceptor-substituted porphyrins. *Angewandte Chemie International Edition*. 2010; **49**(37):6646-6649
- [12] Schiffmann F, VandeVondele J, Hutter J, Urakawa A, Wirz R, Baiker A. An atomistic picture of the regeneration process in dye sensitized solar cells. *Proceedings of the National Academy of Sciences*. 2010;**107**(11):4830-4833
- [13] Nazeeruddin MK, Kay A, Rodicio I, Humphry-Baker R, Müller E, Liska P, et al. Conversion of light to electricity by cis-X₂bis (2, 2'-bipyridyl-4, 4'-dicarboxylate) ruthenium (II) charge-transfer sensitizers (X= Cl-, Br-, I-, CN-, and SCN-) on nanocrystalline titanium dioxide electrodes. *Journal of the American Chemical Society*. 1993; **115**(14):6382-6390
- [14] Yu Q, Wang Y, Yi Z, Ningning Z, Zhang J, Zhang M, et al. High-efficiency dye-sensitized solar cells: The influence of lithium ions on exciton dissociation, charge recombination, and surface states. *ACS Nano*. 2010;**4**(10): 6032-6038
- [15] Duan C, Huang F, Cao Y. Recent development of push-pull conjugated polymers for bulk-heterojunction photovoltaics: Rational design and fine tailoring of molecular structures. *Journal of Materials Chemistry*. 2012;**22**(21): 10416-10434

- [16] Chen G, Sasabe H, Igarashi T, Hong Z, Kido J. Squaraine dyes for organic photovoltaic cells. *Journal of Materials Chemistry A*. 2015;**3**(28): 14517-14534
- [17] Xunjin ZHU, Chen S, Wong WY, Wong WK. Design and synthesis of porphyrin materials for highly efficient organic photovoltaics. U.S. Patent Application 15/635,563. 2018
- [18] Suarez M, Patricia Avila-Torres Y, Caicedo C, Guateque J, Florez-Lopez E. Novel macrocyclic thiazole as potential organic photovoltaic. In: *Proceedings of the 10 th European meeting on Solar Chemistry and Photocatalysis: Environmental Applications (SPEA10)*. 2018. pp. 626-628
- [19] Frisch MJE, Trucks GW, Schlegel HB, Scuseria GE, Robb MA, Cheeseman JR, et al. Gaussian 09, Revision a. 02. Wallingford, CT: Gaussian, Inc.; 2009. p. 200
- [20] Hohenberg P, Kohn W. Inhomogeneous electron gas. *Physical Review*. 1964;**136**:B864
- [21] Kohn W, Sham LJ. Self-consistent equations including exchange and correlation effects. *Physical Review*. 1965;**140**:A1133
- [22] ASTM G. 173-03: Standard Tables for Reference Solar Spectral Irradiances: Direct Normal and Hemispherical on 37 Tilted Surface. West Conshohocken, PA: ASTM International; 2003
- [23] Lee C, Yang W, Parr RG. Development of the Colle-Salvetti correlation-energy formula into a functional of the electron density. *Physical Review B*. 1988;**37**:785
- [24] Williams RM, De Cola L, Hartl F, Lagref JJ, Planeix JM, De Cian A, et al. Photophysical, electrochemical and electrochromic properties of copper-bis (4, 4'-dimethyl-(3,2), 6, 6'-diphenyl-2, 2'-bipyridine) complexes. *Coordination Chemistry Reviews*. 2002;**230**:253-261
- [25] Lee S, Seok CH, Park Y, Lee A, Jung DH, Choi SH, et al. Enforced effects of side group substitution position on luminescence properties; synthesis of Bis (dipyrinato) zinc complex derivatives. *Molecular Crystals and Liquid Crystals*. 2010;**531**: 65-365
- [26] Fitri A, Benjelloun AT, Benzakour M, Mcharfi M, Hamidi M, Bouachrine M. Theoretical design of thiazolothiazole-based organic dyes with different electron donors for dye-sensitized solar cells. *Spectrochimica Acta Part A: Molecular and Biomolecular Spectroscopy*. 2014;**132**: 232-238
- [27] Nazeeruddin MK, Pechy P, Renouard T, Zakeeruddin SM, Humphry-Baker R, Comte P, et al. Engineering of efficient panchromatic sensitizers for nanocrystalline TiO₂-based solar cells. *Journal of the American Chemical Society*. 2001; **123**(8):1613-1624
- [28] Gao F, Wang Y, Dong S, Zhang J, Wang M, Jing X, et al. Enhance the optical absorptivity of nanocrystalline TiO₂ film with high molar extinction coefficient ruthenium sensitizers for high performance dye-sensitized solar cells. *Journal of the American Chemical Society*. 2008;**130**(32):10720-10728
- [29] Chen C-Y, Wang M, Li J-Y, Pootrakulchote N, Alibabaei L, Ngoc-le C-h, et al. Highly efficient light-harvesting ruthenium sensitizer for thin-film dye-sensitized solar cells. *ACS Nano*. 2009;**3**(10):3103-3109
- [30] Swetha T, Niveditha S, Bhanuprakash K, Singh SP. Panchromatic Ru (II) Dipyrins as NCS free sensitizers showing highest efficiency for DSSCs. *Electrochimica Acta*. 2015;**153**:343-351

- [31] Naik P, Elmorsy MR, Rui S, Babu DD, El-Shafei A, Adhikari AV. New carbazole based metal-free organic dyes with D- π -A- π -a architecture for DSSCs: Synthesis, theoretical, and cell performance studies. *Solar Energy*. 2017;**153**:600-610
- [32] Dayan S, Özpozan NK. Performance improvement of RuII complexes pyridinyl backbone on dye-sensitized solar cells (DSSC). *Inorganica Chimica Acta*. 2018;**474**:81-88
- [33] Lyu S, Bertrand C, Hamamura T, Ducasse L, Toupance T, Olivier C. Molecular engineering of ruthenium-diacetylide organometallic complexes towards efficient green dye for DSSC. *Dyes and Pigments*. 2018;**158**:326-333
- [34] Hsieh C-P, Lu H-P, Chiu C-L, Lee C-W, Chuang S-H, Mai C-L, et al. Synthesis and characterization of porphyrin sensitizers with various electron-donating substituents for highly efficient dye-sensitized solar cells. *Journal of Materials Chemistry*. 2010;**20**(6):1127-1134
- [35] Yella A, Lee H-W, Tsao HN, Yi C, Chandiran AK, Nazeeruddin MK, et al. Porphyrin-sensitized solar cells with cobalt (II/III)-based redox electrolyte exceed 12 percent efficiency. *Science*. 2011;**334**(6056):629-634
- [36] Yella A, Mai C-L, Zakeeruddin SM, Chang S-N, Hsieh C-H, Yeh C-Y, et al. Molecular engineering of push-pull porphyrin dyes for highly efficient dye-sensitized solar cells: The role of benzene spacers. *Angewandte Chemie International Edition*. 2014;**53**(11):2973-2977
- [37] Mathew S, Yella A, Gao P, Humphry-Baker R, Curchod BFE, Ashari-Astani N, et al. Dye-sensitized solar cells with 13% efficiency achieved through the molecular engineering of porphyrin sensitizers. *Nature Chemistry*. 2014;**6**(3):242
- [38] Duanglaor P, Thiampanya P, Sudyoadsuk T, Promarak V, Pulpoka B. Synthesis and photophysical properties of donor-acceptor system based bipyridylporphyrins for dye-sensitized solar cells. *Journal of Energy Chemistry*. 2015;**24**(6):779-785
- [39] Prakash K, Manchanda S, Sudhakar V, Sharma N, Sankar M, Krishnamoorthy K. Facile synthesis of β -functionalized "push-pull" Zn (II) porphyrins for DSSC applications. *Dyes and Pigments*. 2017;**147**:56-66
- [40] Martín-Gomis L, Parejo C, Álvarez JC, Fernández-Lázaro F, Sastre-Santos Á. Dye sensitized solar cells (DSSCs) based on bulky tert-octylphenoxy-carboxyphenyl substituted phthalocyanine without the presence of co-adsorbents. *Inorganica Chimica Acta*. 2017;**468**:327-333
- [41] Hara K, Tachibana Y, Ohga Y, Shinpo A, Suga S, Sayama K, et al. Dye-sensitized nanocrystalline TiO₂ solar cells based on novel coumarin dyes. *Solar Energy Materials and Solar Cells*. 2003;**77**(1):89-103
- [42] Hara K, Kurashige M, Dan-oh Y, Kasada C, Shinpo A, Suga S, et al. Design of new coumarin dyes having thiophene moieties for highly efficient organic-dye-sensitized solar cells. *New Journal of Chemistry*. 2003;**27**(5):783-785
- [43] Hagberg DP, Edvinsson T, Marinado T, Boschloo G, Hagfeldt A, Sun L. A novel organic chromophore for dye-sensitized nanostructured solar cells. *Chemical Communications*. 2006;**21**:2245-2247
- [44] Wang Z-S, Cui Y, Dan-oh Y, Kasada C, Shinpo A, Hara K. Thiophene-functionalized coumarin dye for efficient dye-sensitized solar cells: Electron lifetime improved by coadsorption of deoxycholic acid. *The Journal of Physical Chemistry C*. 2007;**111**(19):7224-7230

- [45] Ito S, Miura H, Uchida S, Takata M, Sumioka K, Liska P, et al. High-conversion-efficiency organic dye-sensitized solar cells with a novel indoline dye. *Chemical Communications*. 2008;**41**:5194-5196
- [46] Zeng W, Cao Y, Yu B, Wang Y, Shi Y, Zhang M, et al. Efficient dye-sensitized solar cells with an organic photosensitizer featuring orderly conjugated ethylenedioxythiophene and dithienosilole blocks. *Chemistry of Materials*. 2010;**22**(5):1915-1925
- [47] Bai Y, Zhang J, Zhou D, Wang Y, Zhang M, Wang P. Engineering organic sensitizers for iodine-free dye-sensitized solar cells: Red-shifted current response concomitant with attenuated charge recombination. *Journal of the American Chemical Society*. 2011;**133**(30): 11442-11445
- [48] Tsao HN, Yi C, Moehl T, Yum J-H, Zakeeruddin SM, Nazeeruddin MK, et al. Cyclopentadithiophene bridged donor-acceptor dyes achieve high power conversion efficiencies in dye-sensitized solar cells based on the tris-cobalt bipyridine redox couple. *ChemSusChem*. 2011;**4**(5):591-594
- [49] Kakiage K, Aoyama Y, Yano T, Oya K, Fujisawa J-i, Hanaya M. Highly-efficient dye-sensitized solar cells with collaborative sensitization by silyl-anchor and carboxy-anchor dyes. *Chemical Communications*. 2015; **51**(88):15894-15897
- [50] Narayanaswamy K, Swetha T, Kapil G, Pandey SS, Hayase S, Singh SP. Simple metal-free dyes derived from triphenylamine for DSSC: A comparative study of two different anchoring group. *Electrochimica Acta*. 2015;**169**:256-263
- [51] Massin J, Ducasse L, Abbas M, Hirsch L, Toupance T, Olivier C. Molecular engineering of carbazole-fluorene sensitizers for high open-circuit voltage DSSCs: Synthesis and performance comparison with iodine and cobalt electrolytes. *Dyes and Pigments*. 2015;**118**:76-87
- [52] Capodilupo AL, De Marco L, Corrente GA, Giannuzzi R, Fabiano E, Cardone A, et al. Synthesis and characterization of a new series of dibenzofulvene based organic dyes for DSSCs. *Dyes and Pigments*. 2016;**130**: 79-89
- [53] Demeter D, Melchiorre F, Biagini P, Jungsuttiwong S, Po R, Roncali J. 3, 4-Ethylenedioxythiophene (EDOT) and 3, 4-ethylenedithiathiophene (EDTT) as terminal blocks for oligothiophene dyes for DSSCs. *Tetrahedron Letters*. 2016; **57**(43):4815-4820
- [54] Liao Y, Hu J, Zhu C, Liu Y, Xu C, Chen C, et al. Synthesis and photovoltaic performance of novel polymeric metal complex sensitizer with benzodithiophene or carbazole derivative as donor in dye-sensitized solar cell. *Journal of Molecular Structure*. 2016;**1108**:467-474
- [55] Park K-W, Serrano LA, Ahn S, Baek MH, Wiles AA, Cooke G, et al. An investigation of the role the donor moiety plays in modulating the efficiency of 'donor- π -acceptor- π -acceptor' organic DSSCs. *Tetrahedron*. 2017;**73**(8):1098-1104
- [56] Chiu KY, Tran TTH, Chang SH, Yang T-F, Yuhlong Oliver S. A new series of azobenzene-bridged metal-free organic dyes and application on DSSC. *Dyes and Pigments*. 2017;**146**: 512-519
- [57] Elmorsy MR, Rui S, Fadda AA, Etman HA, Tawfik EH, El-Shafei A. Molecular engineering and synthesis of novel metal-free organic sensitizers with D- π -A- π -a architecture for DSSC applications: The effect of the anchoring group. *Dyes and Pigments*. 2018;**158**: 121-130

[58] Pati PB, Yang W, Zade SS. New dyes for DSSC containing triphenylamine based extended donor: Synthesis, photophysical properties and device performance. *Spectrochimica Acta Part A: Molecular and Biomolecular Spectroscopy*. 2017;**178**:106-113

[59] Fattori A, Majer R, Mazzanti A, Ottaviani MF, Modelli A, Mantellini F, et al. N-heterocyclic linkers from 1, 2-diaza-1, 3-dienes for dye-sensitized solar cells: DFT calculations, synthesis and photovoltaic performance. *Dyes and Pigments*. 2017;**145**:246-255

[60] Zhang K, Zhang W, Huang J, Pang A, Wong MS. Metal-free photosensitizers based on benzodithienothiophene as π -conjugated spacer for dye-sensitized solar cells. *Organic Electronics*. 2017;**42**:275-283

[61] Rajavelu K, Sudip M, Kothandaraman R, Rajakumar P. Synthesis and DSSC application of triazole bridged dendrimers with benzoheterazole surface groups. *Solar Energy*. 2018;**166**:379-389

[62] Fernandes SSM, Pereira A, Ivanou D, Mendes A, Manuela M, Raposo M. Benzothiadiazole derivatives functionalized with two different (hetero) aromatic donor groups: Synthesis and evaluation as TiO_2 sensitizers for DSSCs. *Dyes and Pigments*. 2018;**151**:89-94

[63] Naik P, Babu DD, Rui S, El-Shafei A, Adhikari AV. Synthesis, characterization and performance studies of a new metal-free organic sensitizer for DSSC application. *Materials Today: Proceedings*. 2018; **5**(1):3150-3157

[64] Suarez M, Carolina C, Jimmy M, Edwin F-L, Yenny Á-T. Design, theoretical study and correlation of the electronic and optical properties of diethynylphenylthiophene as photovoltaic materials. *Journal of Molecular Structure*. 2020;**1201**:127093